Surface conductivity of Mercury provides current closure and may affect magnetospheric symmetry

P. Janhunen and E. Kallio

Finnish Meteorological Institute, Geophysical Research, Helsinki, Finland

Surface conductivity of Mercury provides current closure and may affect magnetospheric symmetry

P. Janhunen and E. Kallio

Finnish Meteorological Institute, Geophysical Research, Helsinki, Finland

Abstract. We study what effect a possible surface conductivity of Mercury has on the closure of magnetospheric currents by making six runs with a quasineutral hybrid simulation. The runs are otherwise identical but use different synthetic conductivity models: run 1 has fully conducting planet, run 2 has poorly conducting planet ($\sigma = 10^{-8}\Omega^{-1}\,\text{m}^{-1}$) and runs 3-6 have one of the hemispheres either in dawn-dusk or day-night directions well conducting, the other one being poorly conducting. Although the surface conductivity is not known from observations, educated guesses easily give such conductivity values that magnetospheric currents may close partly within the planet and as the conductivity depends heavily on the mineral composition of the surface, the possibility of significant horizontal variations cannot be easily excluded. The simulation results show that strong horizontal variations may produce modest magnetospheric asymmetries. Beyond the hybrid simulation, we also briefly discuss the possibility that in the nightside there may be a lack of surface electrons to carry downward current which may act as a further source of surface-related magnetospheric asymmetry.

1 Introduction

The structure of Mercury's magnetosphere and especially the mechanisms by which it interacts with the solar wind and the planet are still largely unknown. It has been known for 30 years since Mariner-10 that the planet has an intrinsic magnetic field (Ness et al., 1974; Simpson et al., 1974). Later it was found using ground-based measurements that the planet has an extended exosphere containing at least sodium and potassium (Potter and Morgan, 1997). The Mariner-10 data have also given rise to the interpretation that an intense substorm-like field-aligned current (FAC) system of ~ 1.4 MA magnitude exists sporadically (Slavin et al., 1997). This magnitude of the current is comparable to the FAC systems found in Earth's magnetosphere.

The closure mechanism of FAC systems, especially if they are as large as ~ 1.4 MA, has remained mysterious (Slavin

et al., 1997; Glassmeier, 2000). The atmosphere of Mercury is so tenuous that the exosphere extends all the way to the planet (Killen and Ip, 1999). The height-integrated dayside Pedersen conductivity Σ_P due to exospheric Na^+ pickup has been estimated as 0.1 S (Cheng et al., 1987) which, although not completely negligible, is probably too small to provide significant FAC closure. For comparison, in the Earth's ionosphere Σ_P is typically 10 S.

The subject of this paper is to study the effect of the planetary conductivity on the FAC closure and the structure of the magnetosphere by making a series of runs with a quasineutral hybrid simulation. In Section 2 we consider current closure within Mercury using simple analytical models, then present the quasineutral hybrid simulation model (Section 3) and then the simulation results (Section 4). We close the paper with discussion (Section 5) and summary (Section 6).

2 Theoretical preliminaries

Glassmeier (1997) made an attempt to estimate the effective height-integrated conductivity Σ of the planetary surface based on measured conductivities of lunar samples. If the planetary conductivity is uniform, the penetration depth of the planetary currents is given by the electromagnetic skin depth $\delta = \sqrt{2/(\mu_0\omega\sigma)}$ where μ_0 is the vacuum permeability, ω the angular frequency and σ the conductivity. The height-integrated conductivity is thus $\Sigma \approx \delta\sigma$, i.e.,

$$\Sigma \approx \sqrt{\frac{2\sigma}{\mu_0\omega}}. \qquad (1)$$

Assuming that a typical timescale τ is given by the solar wind travel time across the dayside magnetosphere with extent $\approx 1.5R_P$ ($R_P = 2440$ km is Mercury's radius), we obtain $\tau = 10$ s, i.e. the same value as used by Glassmeier (1997). Selecting a baseline conductivity value as $\sigma = 10^{-4}$ S m^{-1} we obtain $\Sigma = 16$ S, which should already be enough to provide significant FAC closure. The range of conductivity values used by Glassmeier (1997) ranged from 10^{-9} S

m^{-1} (Dyal et al., 1974) to 10^3 S m^{-1} (magnetite at 300 K, (Parkinson and Hutton, 1989)), i.e. 12 decades, corresponding to six decades of Σ from 0.05 S to 50,000 S.

We believe that the lower limit of $\Sigma = 0.05$ S corresponding to $\sigma = 10^{-9}$ S m^{-1} is not realistic for Mercury because then the skin depth corresponding to $\tau = 10$ s is huge, 20 R_P, and we know that the conductivity increases downward because of the temperature increase; at least the hot iron core should be very well conducting. In a steady state ($\omega = 0$), the closure current within the planet selects a path which minimises ohmic heating. For example, consider a two-dimensional (2-D) two-layer steady state model with an upper layer (conductivity σ, thickness H) and a semi-infinite perfect conductor as a lower layer (Figure 1). Assume that the FACs are infinite sheets so that nothing depends on the coordinate perpendicular to the page and also make the simplifying assumptions $L \gg R \gg H$ where L is the horizontal distance of the FAC sheets and R is their thickness. The current goes down vertically below the the FAC input region, flows horizontally on the surface of the ideal conductor and finally moves up to make the upgoing FAC. The total potential difference

$$V = 2E_{\parallel}H = 2\frac{j_{\parallel}H}{\sigma} \qquad (2)$$

where $j_{\parallel}$ is the FAC density (A m^{-2}) and $E_{\parallel}$ is the electric field below the FAC insertion point within the upper layer: only the vertical current in the upper layer contributes to V since the other layer is a perfect conductor. Current continuity implies that the horizontal surface current on the ideal conductor is $J_{\text{hor}} = j_{\parallel}R$ (A m^{-1}) where $j_{\parallel}$ is the FAC density (A m^{-2}). Comparison with the height-integrated "ionospheric Ohm's law" $J_{\text{hor}} = \Sigma E = \Sigma V/L$ then gives

$$\Sigma = \frac{L}{V}J_{\text{hor}} = \frac{L}{V}j_{\parallel}R = \frac{RL}{2H}\sigma \qquad (3)$$

where Eq. (2) was used. Thus, in this example the effective height-integrated conductivity Σ depends on the geometry of the FAC system through the product RL. By varying the assumptions, different dependencies would result, but the bottom line is that Σ is in general geometry-dependent. The case with Earth's ionosphere is different: the insulating atmosphere prohibits magnetospheric currents from closing in the ground, so the horizontal closure currents flow only in the ionosphere. Consequently, for the Earth the height-integrated conductivity is basically independent of the current system geometry: $\Sigma \sim H\sigma$ where H is the thickness of the ionospheric current-carrying layer and σ is ionospheric conductivity, provided only that the scale size of the current system is much larger than H so that the planar approximation for the ionosphere is valid. For Mercury, as we saw above, the currents can flow anywhere in the planet and thus the height-integrated conductivity is geometry-dependent also when the spatial scale of the current system is large.

3 Simulation model

Our quasineutral hybrid simulation code is described in Kallio and Janhunen (2003a). In a quasineutral hybrid simulation, ions are treated as particles and electrons as a charge-neutralising fluid. Run 1 (Table 1) in this paper is otherwise identical to the baseline run (conducting planet) reported in that paper except that a three-level hierarchically adapted octogrid is used to speed up the computation and increase the accuracy near the planet (a uniform grid was used in Kallio and Janhunen (2003a)). The largest grid spacing is $1/4R_M$, the first adaptation is $1/8R_M$ and the second (finest) adaptation level is $1/16R_M$ (153 km). We use a coordinate system where X points towards Sun, Z is northward antiparallel to the planet's dipole moment vector and Y completes the right-handed coordinate system, pointing from dawn to dusk. The solar wind is assumed to be proton plasma having density 76 cm^{-3}, velocity 430 km s^{-1} in $-X$ direction and 10 nT interplanetary magnetic field (IMF) in $+Z$ direction (i.e., northward IMF and closed magnetosphere). In runs 2-6, a poorly conducting region is set up in different parts of the planet (Table 1). In run 2 the whole planet has a low conductivity of $10^{-8}\Omega^{-1}$ m^{-1}. In runs 3-6 half of the planet has a low conductivity of $5 \times 10^{-9}\Omega^{-1}$ m^{-1}, the other half being well conducting. We estimate that the conductivity is $\sim 10^{-4}\Omega^{-1}$ m^{-1} due to numerical diffusion in the well conducting regions. In order to obtain an estimate of the maximal effect of conductivity changes, the conductivity of the poorly conducting regions is set to a value ($\sim 10^{-8}\Omega^{-1}$ m^{-1}) which is close to the lower limit of the physically reasonable values.

4 Simulation results

4.1 Current closure in the planet

In Figure 2 we show the colour-coded current density (A m^{-2}) entering (red) and exiting (blue) the planet at the surface in all six runs. In all cases, since there is no dipole tilt and the IMF B_x and B_y are assumed zero, the northern and southern hemispheres are symmetric apart from numerical noise whose effect is minor in this representation. We remark that while the symmetry in the north-south direction depends on the symmetry of the boundary conditions, there is always a dawn-dusk asymmetry in a quasineutral hybrid model due to finite Larmor radius effects and furthermore, IMF B_x also causes north-south asymmetry [Kallio and Janhunen (2003c), Figure 1]. In run 1 (conducting planet), the main feature is the existence of "Region-1" current systems at $\sim 30^{\circ}$ latitude. A comparison with proton impact maps computed from the same simulation code (Kallio and Janhunen, 2003b) shows that on the nightside the Region-1 current system is approximately colocated with a region of enhanced proton precipitation while on the dayside the main proton impact region is located on the poleward side of the current system. In the duskside (dawnside) the current is out of (into) the planet. Close to noon there are "cusp-related"

current systems at higher latitude ($\sim 60°$). On both sides of the midnight, the duskside and dawnside Region-1 currents partly overlap: on the duskside (dawnside) near midnight there is some upward (downward) current on the poleward (equatorward) side of the main Region-1 current. In the dawnside this "anti-Region-1" current has the same sense and relative location as the Region-2 current in Earth's magnetosphere, but on the duskside this interpretation breaks down because the Region-2 should be on the equatorward side of the Region-1 and not on its poleward side as in Fig. 2. In the other runs, the features are similar except that in poorly conducting regions the currents are much weaker and more irregular.

Let us define the single-hemisphere upward and downward total currents by

$$
\begin{aligned}
I_{\text{up}} &= +\frac{1}{2}\int_{(4\pi)} dS\, \max(0, j) \\
I_{\text{down}} &= -\frac{1}{2}\int_{(4\pi)} dS\, \min(0, j),
\end{aligned}
\tag{4}
$$

where j is the radial current density shown in Fig. 2, i.e. only positive (negative) radial current contributes to I_{up} (I_{down}). The integrals extend over the whole planet but the factor $1/2$ ensures that I_{up} and I_{down} are effectively for one hemisphere only. Both I_{up} and I_{down} are positive quantities.

Single-hemisphere total currents I are listed in Table 2, where I is computed as

$$
I = \frac{1}{2}\left(I_{\text{up}} + I_{\text{down}}\right).
\tag{5}
$$

Current I flows down and up through one of the hemispheres, computed as an average of both hemispheres to reduce numerical noise. A $\pm$ error estimate ΔI is also given in Table 2, which is defined as

$$
\Delta I = \frac{1}{2}\left|I_{\text{up}} - I_{\text{down}}\right|.
\tag{6}
$$

The error is not significant and its source is numerical interpolation. The third column of Table 2 is the current computed in a grid which is two times coarser than the grid shown in Fig. 2. When the grid is coarsened, the currents decrease relatively more in the runs having poor conductivity, which suggests that the current is not only weaker but its pattern has more small-scale features when the underlying surface is poorly conducting. The total current for the coarser grid and poorly conducting planet (0.29 MA) is of the same order of magnitude as the 0.1 MA obtained by Ip and Kopp (2003) using an MHD simulation.

4.2 Current lines in the magnetosphere

Figure 3 shows lines of magnetospheric current density followed from the duskside planetary surface at points where the current out of the planet is significant. Most of the current lines make a turn at $X \approx 0$ magnetopause and return to the dawnside of the planet. This behaviour is very reminiscent to the shape of the closure path of Region-1 FAC systems in Earth's magnetosphere as found from global magnetohydrodynamic (MHD) simulations (Tanaka, 1995; Janhunen and Koskinen, 1997). That one sees a similar feature in a different planet using a different simulation technique insinuates that the geometry of the closure path of Region-1 currents is a robust feature of terrestrial planet magnetospheres.

4.3 XZ plane current density

Figure 4 shows the y component of the current density in the XZ plane in all six runs. Red and blue correspond to positive and negative j_y, respectively, and y is positive from dawn to dusk. In run 1 (fully conducting planet), the Chapman-Ferraro (C-F) current is seen as red near the subsolar point at $z \approx 0$ and as blue branches at larger $|z|$. At higher x (more towards the sun), a weaker intensity bow shock current (red) is seen, which is similar in all six runs. The conducting planet is surrounded by a surface current which is visible as a narrow red ring. Near the cusp, the surface current turns negative (blue) and at the same time a red current flows in the plasma near the planet. The latter current transforms continuously to the red surface current. It is not clear if this red current should be interpreted as being a disconnected branch of the C-F current or some other current system. In the nightside, the tail current sheet is clearly seen as red. The inner edge of the tail current sheet is bifurcated (a "snake's tongue"). A similarly bifurcated inner edge of the tail current is routinely seen in MHD simulations of the Earth's magnetosphere using our global MHD code GUMICS-4 (Palmroth et al., 2001, for example). This is a second example of a robust feature seen in different terrestrial planets using different simulation techniques.

In run 2 (Figure 4, top right, poorly conducting planet), the red C-F current has a shape which differs from run 1. All currents now flow basically outside the planet. The tail current sheet extends to closer distance as in run 1. Near the surface, current structuring is seen, especially at middle latitudes.

In run 3 (Figure 4, middle row, left, poorly conducting dayside and well conducting nightside), the nightside and dayside are similar to run1 and run 2, respectively: the current systems do not much extend over the terminator ($x = 0$) but instead they mainly close separately in nightside and dayside. Some interaction exists, as at the conductivity gradient ($x = 0$) there are some currents also deep inside the planet.

Run 4 (Figure 4, middle row, right) has a poorly conducting nightside and well conducting dayside. Again the nightside and dayside are similar to the corresponding homogeneous conductivity runs (for the nightside, run 2, for the dayside, run 3). In the nightside, however, the tail current sheet does not extend quite so close to the planet as in run 2.

In runs 5 and 6 (Figure 4, bottom row) the conductivity has an evening-morning asymmetry. The expected asymmetries are easier to discuss in the XY plane, which we do next.

4.4 XY plane magnetic field

In Figure 5 we plot the magnitude of the perturbation magnetic field $B_1 = |\mathbf{B} - \mathbf{B}_{\mathrm{dip}}|$ in the equatorial plane (XY plane) where $\mathbf{B}_{\mathrm{dip}}$ is the dipole field. In all runs there is a rather strong dawn-dusk asymmetry near the bow shock, the magnetic field being stronger in the dawnside ($y < 0$) than in the duskside. Likewise, in all runs the magnetotail is not smooth but exhibits structuring. We checked that the structuring is due to undulations in the tail current sheet; the field in the tail lobes at $z \neq 0$ is smoother. In all cases, the $\mathbf{B}_1$ field penetrates only the poorly conducting parts of the planet as expected. A comparison of runs 5 and 6 (bottom row) shows that more structuring in the magnetotail occurs at the hemisphere which is the poorly conducting one. A poor conductivity inhibits currents from closing within the planet, which leads to more small scale structures developing in the current systems. This resistivity-stimulated small scale structuring is not limited to the regions of the magnetosphere near the planet but also extends its influence to the tail current sheet.

5   Discussion

The conductivity of Mercury's surface may well be in the nontrivial range so that from the magnetosphere current closure point of view, the planet is neither fully conducting nor completely resistive. Furthermore, it is not inconceivable that large horizontal conductivity differences may exist which may cause global asymmetries in the magnetosphere. It is the purpose of this paper to quantify the magnitude of such asymmetries by using a set of rather extreme case models where the conductivity on different sides of the planet differs maximally. The results show that the magnetospheric structure may be changed due to surface conductivity differences, although probably not in a dominant way. When interpreting future data from Mercury, the possible role of the planetary surface as a source of magnetospheric asymmetry should be kept in mind, however.

We emphasise that the height-integrated conductivity which is successfully used to describe Earth's ionosphere is not so viable concept at Mercury because the current is not limited to flow in a layer but may flow anywhere inside the planet where the material is enough conducting. This is reflected by the fact that the value of the height-integrated conductivity depends not only on the surface properties but also on the geometry of the current system (Eq. 3).

Should the planet be resistive enough that no significant current closure in the surface can take place, another conductivity-related effect might become observable: an inductive heating of the planet's interior (Shimazu and Terasawa, 1995). The less conducting the surface is, the deeper the solar wind induced variations penetrate, and the deeper they penetrate, the more effective such heating is in raising the interior temperature because of an increasingly thick thermal blanket. When trying to estimate the possible magnitude of the heating we came into the conclusion that the interior temperature

increase due to inductive heating is likely to be minimal unless the conductivity of the planet is for some reason really low. Thus there is a possibility for conductivity-related effects regardless of what the value of the conductivity turns out to be: either current closure through the surface (more likely), or, if the conductivity is too low for it, inductive heating of the planet's interior (less likely).

Returning to the question of magnetospheric current closure, there are four types of current systems: (1) dayside upward currents, (2) dayside downward currents, (3) nightside upward currents and (4) nightside downward currents. In the dayside, the plasma density is several tens of electrons per cubic centimetre while the maximum surface-normal current density is $\sim 0.5\mu$ A m^{-2} (Fig. 2). This current density can be carried already by the protons impacting the surface (Kallio and Janhunen, 2003b). The electron thermal current is easily much larger, although a detailed estimation is not possible for us as the electrons are not explicitly modelled in the quasineutral hybrid code. Thus on the dayside there is no lack of current carries, but rather there may be need for potential drops or barriers that limit the electron thermal current and negative charging of the planet (see Ip (1986) for an analysis of surface charging).

In the nightside the plasma density is in places as small as 0.1-0.2 cm^{-3} in our simulations while the maximum current density is about the same as on the dayside (0.5μ A m^{-2}). In such tenuous plasma, ions can be neglected as current carriers, unless they are accelerated to several tens of keV energy. The obtained nightside upward currents are probably possible to carry by magnetospheric electrons after they have possibly undergone some potential drop or wave-induced acceleration. The fourth type of current is the nightside downward current. This current is problematic in terms of current carriers: it should be carried by magnetospheric ions (which is very difficult) or by electrons emerging from the surface (which is difficult as well in the nightside where there is no photoionisation). Maybe the current is carried by secondary electrons emitted by ion bombardment or electrons transferred from the dayside. There is yet another possibility, which is relevant for this paper: the system might select to avoid nightside downward currents altogether by shifting the nightside-dawnside part of the "Region-1" current system towards the dayside where there are more current-carrying photoelectrons available. Simulating these electron effects is unfortunately outside the scope of the present quasineutral hybrid simulation. The reason why we bring the issue up here is that it may be an extra source of asymmetry in the magnetosphere which is not related to the planetary conductivity but to the way the magnetosphere interacts with the surface.

6   Summary

We summarise our results briefly:

1. For reasonable educated guesses for Mercury's surface conductivity, magnetospheric currents are expected to

close at least to some extent through the planet in a way which does not have a direct analogy at the Earth because the Earth has an insulating atmosphere whereas on Mercury the conducting plasma is in contact with the more or less conducting surface.

2. A set of hybrid simulation runs shows that horizontal differences in the surface conductivity may be sources of global asymmetries in the magnetosphere.

3. Additional asymmetries might arise from the difficulty to carry downward currents in the nightside due to lack of electrons at the surface. Full particle simulations are probably required to model these electrons effects.

References

Cheng, A.F., R.E. Johnson, S.M. Krimigis and L. Lanzerotti, Magnetosphere, exosphere, and surface of Mercury, *Icarus,* 71, 430–440, 1987.

Dyal, P., C.W. Parkin and W.D. Daily, Magnetism and the interior of the Moon, *Rev. Geophys. Space Phys.,* 12, 568–591, 1974.

Glassmeier, K.-H., The Hermean magnetosphere and its ionosphere–magnetosphere coupling, *Plan. Space Sci.,* 45, 119–125, 1997.

Glassmeier, Currents in Mercury's magnetosphere, in Magnetospheric Current Systems, AGU Geophysical Monograph 118, AGU, 2000.

Ip, W.-H., Electrostatic charging and dust transport at Mercury's surface, *Geophys. Res. Lett.,* 13, 1133–1136, 1986.

Ip, W.-H. and A. Kopp, Mercury's Birkeland current system, *Adv. Space Res.,* in press, 2003.

Janhunen, P. and H.E.J. Koskinen, The closure of Region-1 field-aligned current in MHD simulation, *Geophys. Res. Lett.,* 24, 1419–1422, 1997.

Kallio, E. and P. Janhunen, Modelling the solar wind interaction with Mercury by a quasineutral hybrd model, *Ann. Geophysicae,* in press, 2003a.

Kallio, E. and P. Janhunen, Solar wind and magnetospheric ion impact on Mercury's surface, *Geophys. Res. Lett,* submitted, 2003b.

Kallio, E. and P. Janhunen, The response of the Hermean magnetosphere to the interplanetary magnetic field, *Adv. Space Res.,* in press, 2003c.

Killen, R.M. and W.-H. Ip, The surface-bounded atmospheres of Mercury and the Moon, *Rev. Geophys.,* 37, 361–406, 1999.

Ness, N.F., K.W. Behannon, R.P. Lepping, Y.C. Whang and K.H. Schatten, Magnetic field observations near Mercury: preliminary results from Mariner 10, *Science,* 185, 151–160, 1974.

Palmroth, M., P. Janhunen, T.I. Pulkkinen and W.K. Peterson, Cusp and magnetopause locations in global MHD simulation, *J. Geophys. Res.,* 106, 29435–29450, 2001.

Parkinson, W.D. and V.R.S. Hutton, The electrical conductivity of the Earth, in *Geomagnetism,* ed. J.A. Jacobs, Vol. III, Academic Press, London, 1989.

Potter, A.E. and T.H. Morgan, Evidence for superthermal sodium on Mercury, *Adv. Space Res.,* 19(10), 1571–1576, 1997.

Shimazu, H. and T. Terasawa, Electromagnetic induction heating of meteorite parent bodies by the primordial solar wind, *J. Geophys. Res.,* 100, 16923–16930, 1995.

Simpson, J.A., J.H. Eraker, J.E. Lamport and P.H. Walpole, Electrons and protons accelerated in Mercury's magnetic field, *Science,* 185, 160–166, 1974.

Slavin, J.A., J.C.J. Owen, J.E.P. Connerney and S.P. Christon, Mariner 10 observations of field-aligned currents at Mercury, *Plan. Space Sci.,* 45, 133–141, 1997.

Tanaka, T., Generation mechanisms for magnetosphere-ionosphere current systems deduced from a three-dimensional MHD simulation of the solar wind-magnetosphere-ionosphere coupling processes, *J. Geophys. Res.,* 100, 12057–12074, 1995.

Table 1. Simulation runs

|	
Run 1	Whole planet well conducting, $\sigma \sim 10^{-4}\Omega^{-1}$ m^{-1}
Run 2	Whole planet has $\sigma = 10^{-8}\Omega^{-1}$ m^{-1}
Run 3	Dayside $\sigma = 5 \times 10^{-9}\Omega^{-1}$ m^{-1}, nightside well conducting
Run 4	Nightside $\sigma = 5 \times 10^{-9}\Omega^{-1}$ m^{-1}, dayside well conducting
Run 5	Dawnside $\sigma = 5 \times 10^{-9}\Omega^{-1}$ m^{-1}, duskside well conducting
Run 6	Duskside $\sigma = 5 \times 10^{-9}\Omega^{-1}$ m^{-1}, dawnside well conducting

Table 2. Current closing through one hemisphere

	standard resolution	coarsened
Run 1	(1.40 ± 0.04) MA	1.19 MA
Run 2	(0.40 ± 0.03) MA	0.29 MA
Run 3	(0.97 ± 0.04) MA	0.78 MA
Run 4	(1.05 ± 0.001) MA	0.89 MA
Run 5	(1.27 ± 0.03) MA	1.08 MA
Run 6	(1.13 ± 0.12) MA	0.98 MA
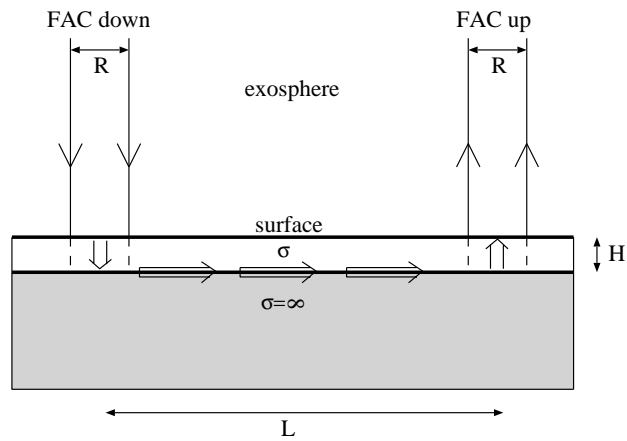
Fig. 1. A schematic 2-D two-layer model for FAC closure. The FAC flows into the surface on the left, moves down across a resistive surface layer (white, conductivity σ) to an ideal conductor surface (gray), where it flows horizontally until it moves up on the right through the resistive layer again and emanates from the surface as an upward FAC.
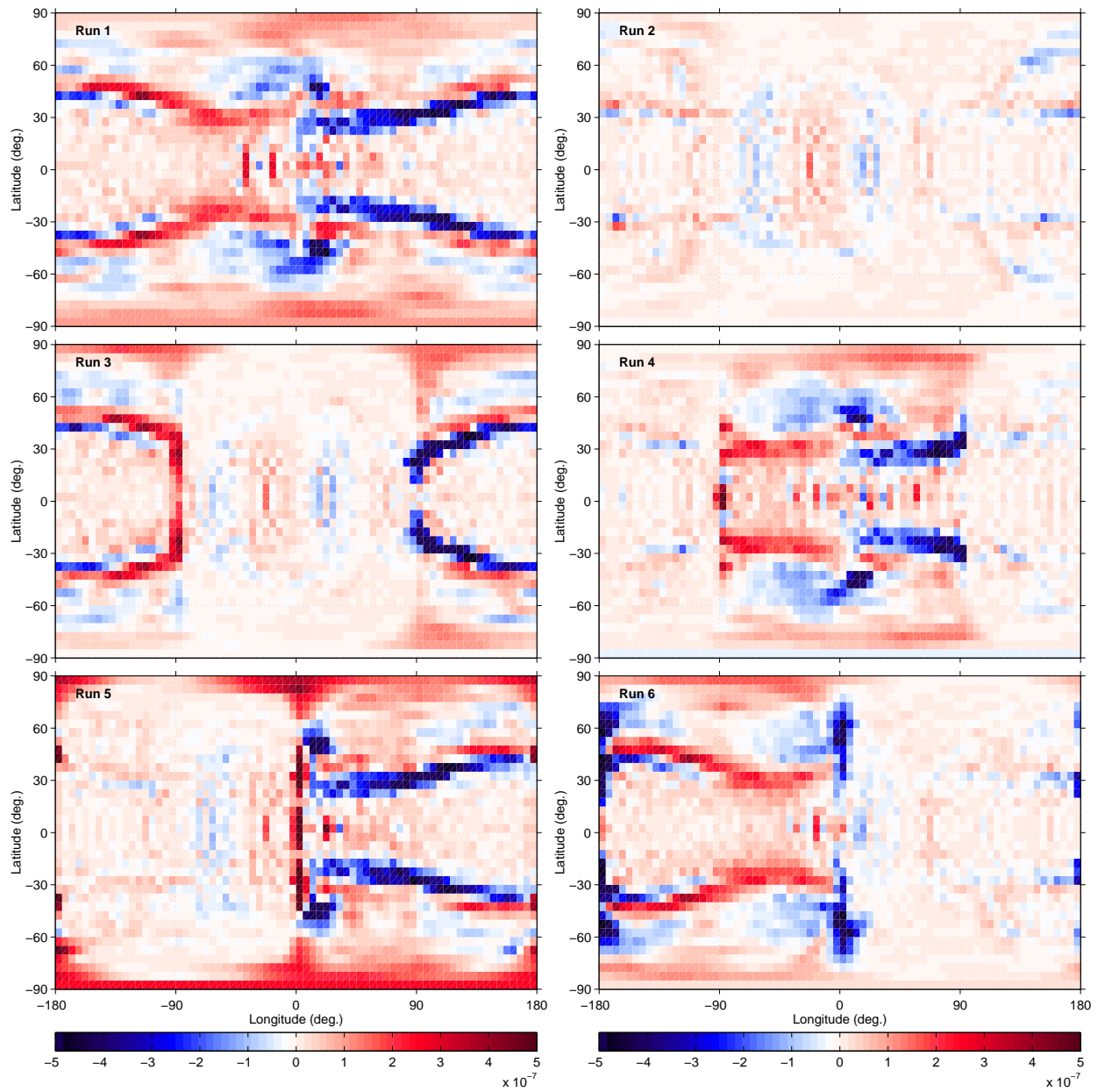
Fig. 2. Current density (A m^{-2}) entering the planet as a function of latitude and longitude in all runs. Zero longitude corresponds to noon and positive longitude to duskside. Positive current (red) is towards the planet and negative (blue) is away from the planet.
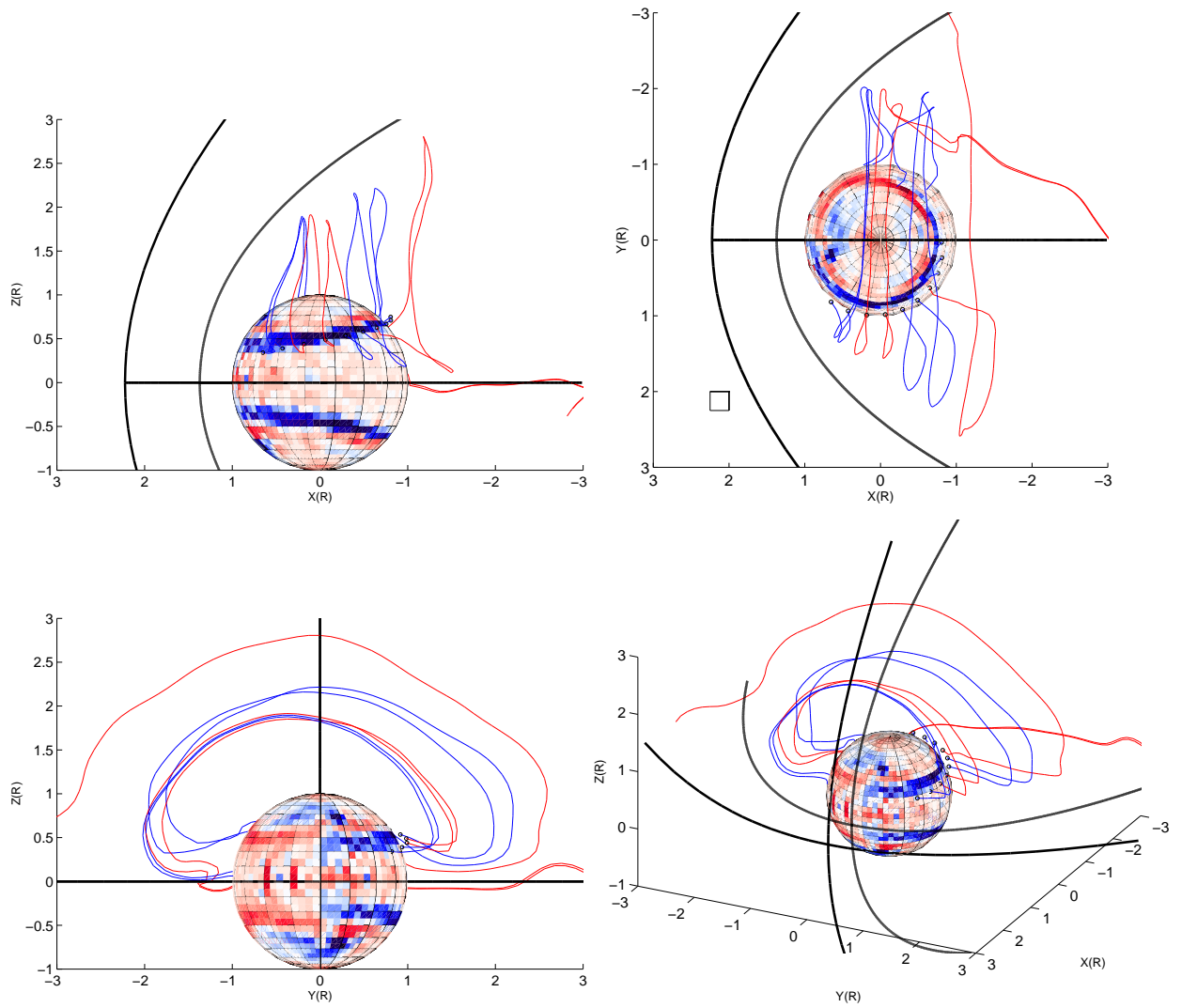
Fig. 3. Current lines starting from the ionosphere for run 1. The same lines are shown from four viewpoints. The starting points are selected in the duskside where significant current flows out of the planet. Lines returning to the planet are shown as blue and lines hitting the simulation box outer boundary are shown are red. To guide the eye, roughly estimated bow shock and magnetopause positions are shown as black lines.
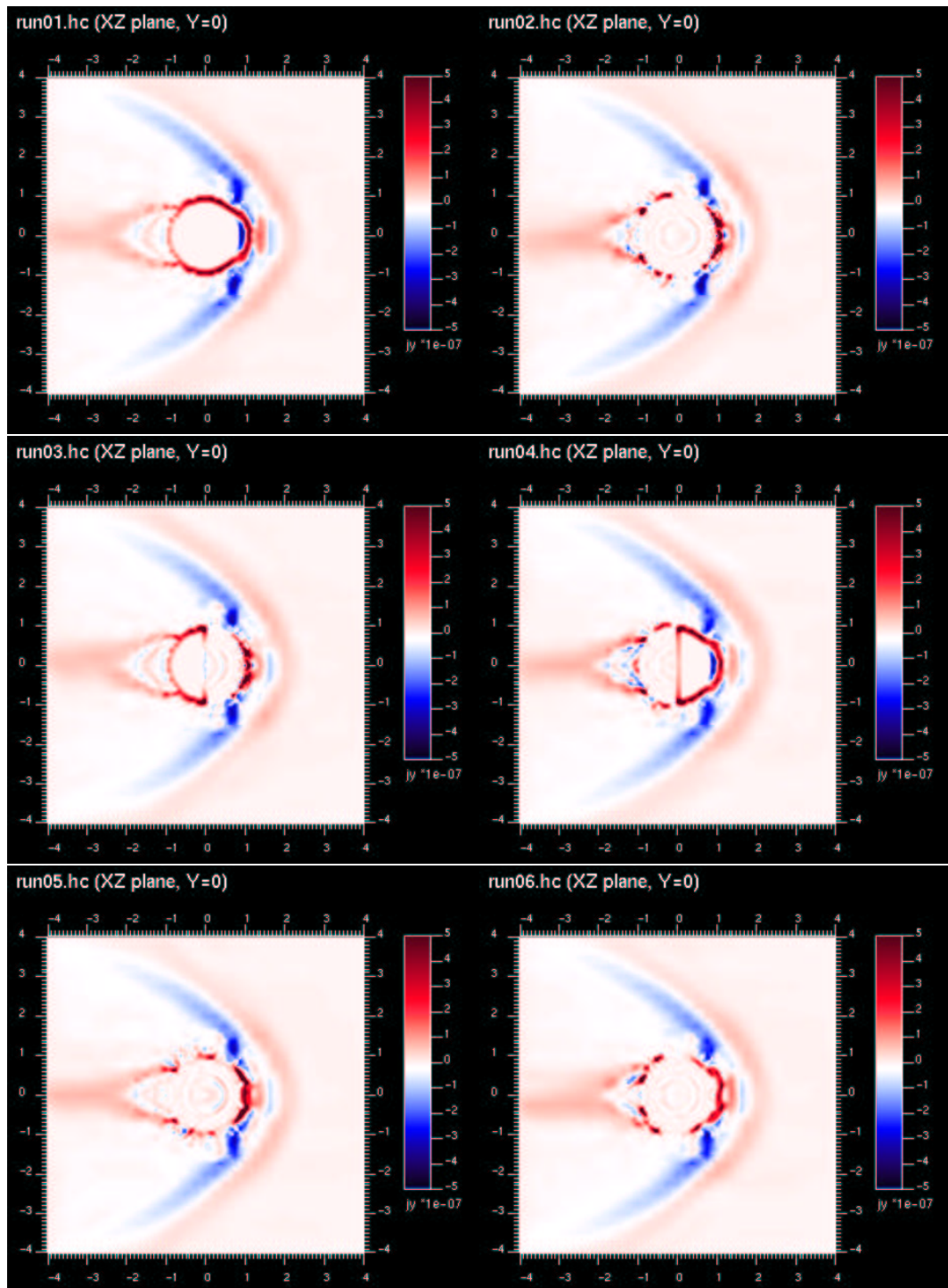
Fig. 4. The current density y component in the XZ plane in all runs (for definitions of runs 1-6, see Table 1). The horizontal axis is X (sun is to the right) and vertical is Z (antiparallel to planetary dipole moment and parallel to IMF). The Y axis points toward the page.
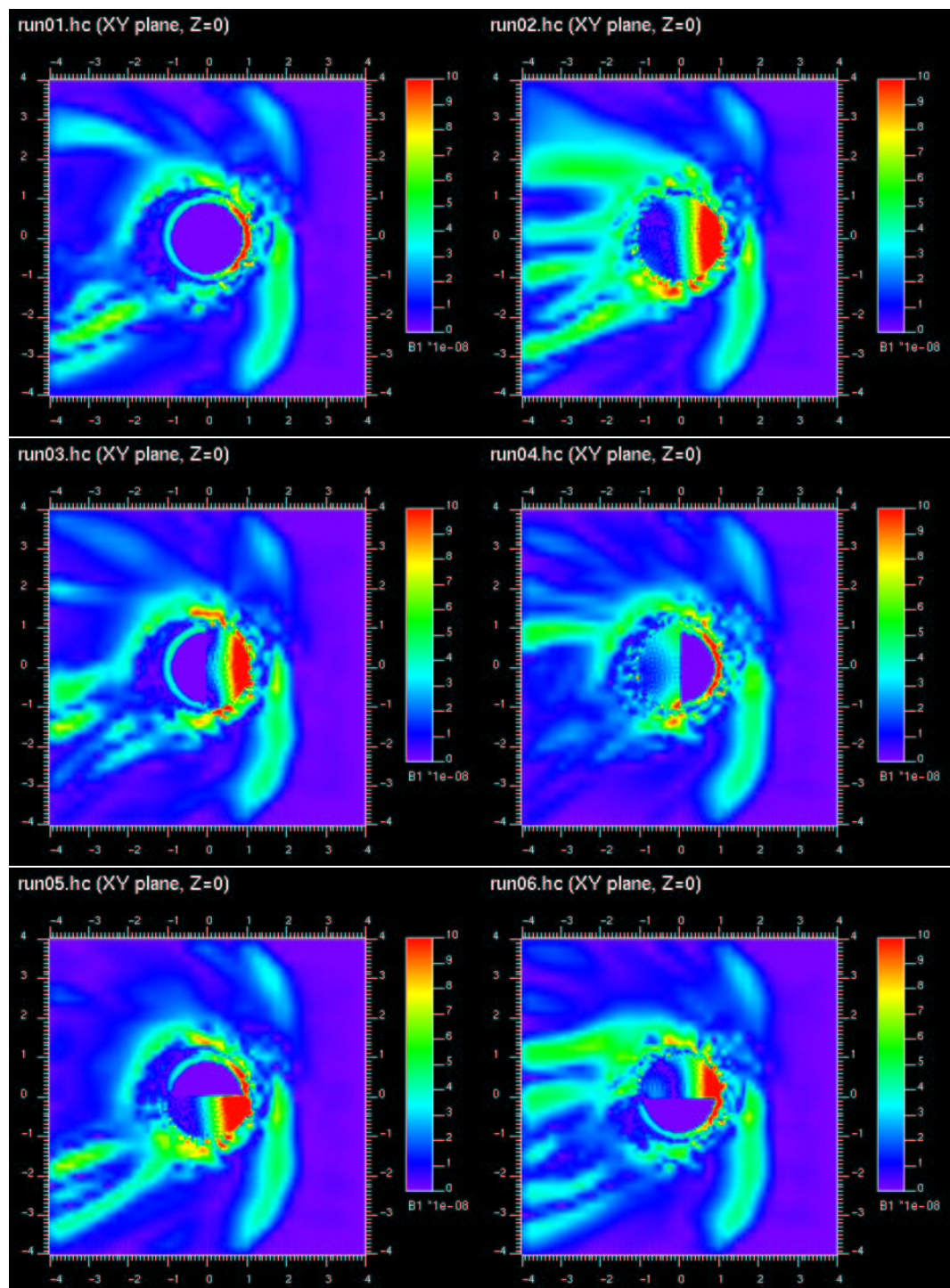
Fig. 5. The perturbation magnetic field $B_1 = |\mathbf{B} - \mathbf{B}_{\mathrm{dip}}|$ in the XY plane in all runs (for definitions of runs 1-6, see Table 1). The horizontal axis is X (sun is to the right) and vertical is Y (growing from dawnside toward duskside). The Z axis points out of the page.